Eur. J. Mech. B/Fluids, **17**, n° 3, 371-384, 1998

Spatio-temporal instability in free ultra-thin films

G. A. SHUGAI * and P. A. YAKUBENKO

ABSTRACT. – The linear evolution of an initially localized disturbance is investigated for a free ultra-thin film of viscous liquid, which is subjected to capillary and long range intermolecular forces. The analysis is based on the long-wave model proposed by Erneux and Davis (1993, *Phys. Fluids A*, **5**, 1117), which is reformulated in an equivalent form by means of the disjoining pressure approach. A negative disjoining pressure due to the van der Waals attraction strongly promotes instability. Both the growth rate along rays $x = Ut$ and speed of the disturbance edges increase as the thickness of the undisturbed film decreases. The estimated film rupture time is larger than that found from linear temporal stability analysis. © Elsevier, Paris.

Keywords. – Thin film, spatio-temporal instability, disjoining pressure.

1. Introduction

Two different approaches are commonly used in continuum theory of ultra thin films (10–100 nm). The first one takes into account the details of long-range intermolecular interactions within the film. Two additional terms may then appear in the equations of motion: the gradient of the van der Waals potential that models the long-range molecular forces (Dzyaloshinskii and Pitaevskii, 1960), and the divergence of the Maxwell stress tensor that represents the electric double-layer repulsion (Felderhof, 1968).

The other simpler approach involves the disjoining pressure concept (Deryagin, 1956). The flow is then governed by the Navier-Stokes equations without any additional terms. Every type of interaction is accounted for completely via the disjoining pressure term in the boundary conditions at the film surfaces. In long-wave theories, both approaches lead to the same result, at least to leading order if applied properly (Maldarelli *et al.*, 1980).

If the van der Waals attraction dominates the double-layer repulsion, the film is unstable. The instability leads to rupture of the film. Linear temporal stability analysis of the flow was performed by Rukenstein and Jain (1974); it was based on the long-wave asymptotic expansion of the Navier-Stokes equations with an extra term due to the van der Waals attraction (see also Maldarelli and Jain, 1988, for a review). Using a similar approach, Erneux and Davis (1993), hereafter referred to as ED, derived a pair of non-linear evolution equations that describe the development of long-wave disturbances. Using further simplifications of these equations, ED and Sharma *et al.* (1995) have performed a weakly non-linear analysis. The latter authors have also studied numerically the fully non-linear development of spatially periodic long-wave disturbances. De Wit *et al.* (1994) have extended the analysis by taking into account insoluble surfactants.

In reality, disturbances are often wave packets localized in space rather than monochromatic waves prescribed by the temporal stability approach. The present linear analysis is a first step in the study of the evolution of wave packets in ultra thin films. It is based on the long-wave approximation suggested by ED. However,

Department of Hydraulic Engineering, The Royal Institute of Technology, S-10044 Stockholm, Sweden
* Correspondence and reprints

0997-7546/98/03/© Elsevier, Paris

their evolution equations are rewritten in an equivalent form by introducing the disjoining pressure instead of the van der Waals potential.

Different stages in the linear spatio-temporal stability analysis of moving "thick" free liquid sheets have been considered by Lin (1981), Lin *et al.* (1990), Li and Tankin (1991), and Li (1993), among others. Most recently, De Luca and Costa (1997) have analyzed the global stability of a spatially developing sheet. A full-scale numerical modelling of spatio-temporal instabilty in a film flowing down a wall was recently performed by Ramaswamy *et al.* (1996). An account of earlier results is contained in the review by Chang (1994).

2. Basic equations

The film is analyzed as a free two-dimensional sheet of Newtonian viscous liquid. The thickness of the undisturbed film is small enough that the long range intermolecular forces are not negligible, yet it is large enough that a continuum theory can be used. The effects of gravity and surrounding medium are assumed to be negligible.

The length scales in the longitudinal (x) and normal (y) directions are chosen as

$$L_x = \varepsilon^{-1}\rho\nu^2\sigma^{-1}, \quad L_y = \rho\nu^2\sigma^{-1}, \tag{2.1}$$

in which ρ is the liquid density, ν is kinematic viscosity, and σ is the surface tension. Furthermore, the thickness of the undisturbed film is assumed to be of order L_y and the typical wavelength of disturbances is of order L_x. If $\varepsilon = L_y/L_x \ll 1$, the long-wave approach can be used.

Since the undisturbed film is motionless, the following scales are used for velocities in the x- and y-directions, respectively:

$$V_x = \varepsilon^{1-\alpha}\rho^{-1}\nu^{-1}\sigma, \quad V_y = \varepsilon^{2-\alpha}\rho^{-1}\nu^{-1}\sigma, \tag{2.2}$$

in which $0 \leq \alpha < 2$. Dimensionless variables are introduced as

$$x = x^* L_x^{-1}, \quad y = y^* L_y^{-1}, \quad t = t^* V_x L_x^{-1}, \tag{2.3}$$

$$h = h^* L_y^{-1}, \quad u = u^* V_x^{-1}, \quad v = v^* V_y^{-1}, \quad p = p^* (\rho V_x^2)^{-1}, \tag{2.4}$$

in which starred symbols stand for corresponding dimensional variables, and h is the film thickness.

The following series expansions are applied:

$$\{u, v, p, h\} = \sum_{j=0}^{\infty} \varepsilon^{(2-\alpha)j} \{u_j, v_j, p_j, h_j\}. \tag{2.5}$$

Two coupled equations that involve only h_0 and u_0 can be derived from the Navier-Stokes equations (see Appendix). One of these equations is

$$\frac{\partial h_0}{\partial t} + \frac{\partial}{\partial x}(u_0 h_0) = 0. \tag{2.6}$$

Two different cases occur for the other equation:

If $\alpha = 0$, it takes the form

$$\frac{\partial u_0}{\partial t} + u_0 \frac{\partial u_0}{\partial x} = \frac{d\Pi}{dh}(h_0) \frac{\partial h_0}{\partial x} + \frac{1}{2} \frac{\partial^3 h_0}{\partial x^3} + \frac{4}{h_0} \frac{\partial}{\partial x} \left(h_0 \frac{\partial u_0}{\partial x} \right), \tag{2.7}$$

in which $\Pi(h)$ is the disjoining pressure, which is made dimensionless by ρV_r^2. If the disjoining pressure can be related to the van der Waals potential only, equations (2.6) and (2.7) are similar to those obtained by ED. Without the disjoining pressure term, they are also known as the Trouton model (e.g. Howell, 1996).

If $\alpha > 0$, (2.7) is replaced by

$$\frac{\partial u_0}{\partial t} + u_0 \frac{\partial u_0}{\partial x} = \frac{d\Pi}{dh}(h_0) \frac{\partial h_0}{\partial x}. \tag{2.8}$$

Equations (2.6) and (2.8) are similar to the shallow water equations.

The most important feature of the above approximation is that both the velocity and pressure are constant across the film. As a consequence, only symmetric disturbances (or squeezing modes) can be investigated (for more details, see Appendix). This restriction is a disadvantage of the present model because antisymmetric disturbances (or stretching modes) can promote the evolution of squeezing modes, even if they do not lead directly to the film rupture. Actually, if the film is being stretched significantly, its thickness decreases due to the mass balance. Smaller thickness of the film in its turn implies increasing of the van der Waals attraction. Furthermore, if stretching disturbances have sufficiently small wavelength and large amplitudes, the film thickness can be non-uniform, which leads to a non-uniform distribution of the disjoining pressure thus providing a possibility of the squeezing modes excitation.

3. Stability analysis

The total flow is decomposed into

$$h_0 = H + h', \quad u_0 = u', \tag{3.1}$$

in which h' and u' are disturbances, and the thickness of the undisturbed film H is made dimensionless by L_y. If the amplitudes of the disturbances are small, (2.6) and (2.7) can be linearized as follows:

$$\frac{\partial h'}{\partial t} + H \frac{\partial u'}{\partial x} = 0, \tag{3.2}$$

$$\frac{\partial u'}{\partial t} = \gamma \frac{\partial h'}{\partial x} + \frac{1}{2} \frac{\partial^3 h'}{\partial x^3} + 4 \frac{\partial^2 u'}{\partial x^2}, \tag{3.3}$$

in which

$$\gamma \equiv \frac{d\Pi_0}{dh}(H). \tag{3.4}$$

If the disturbances are normal modes of the form

$$h' = \tilde{h}\exp(ikx - i\omega t), \quad u' = \tilde{u}\exp(ikx - i\omega t), \tag{3.5}$$

in which $\tilde{h}$ and $\tilde{u}$ are constant amplitudes, then (3.2) and (3.3) yield the dispersion relation

$$D(k,\omega) \equiv (\omega + 2ik^2)^2 - k^2\left[\frac{1}{2}(H-8)k^2 - \gamma H\right] = 0. \tag{3.6}$$

If $\gamma = 0$, (3.6) is similar to the dispersion relation of Lin (1981) for symmetric disturbances in a thick liquid sheet. For $\gamma \leq 0$, no instability occurs. Thus, only the case $\gamma > 0$ is investigated.

If (2.8) is used instead of (2.7), then (3.3) is replaced by

$$\frac{\partial u'}{\partial t} = \gamma\frac{\partial h'}{\partial x}. \tag{3.7}$$

If $\gamma < 0$, (3.2) and (3.7) are similar to the linearized shallow-water equations. The dispersion relation is

$$\omega^2 = -\gamma H k^2. \tag{3.8}$$

If $\gamma \geq 0$, it does not satisfy causality. For $\gamma < 0$, it indicates no instability. Therefore, one needs not to consider this case further.

3.1. Temporal normal mode instability

Dispersion relation (3.6) yields two temporal branches

$$\omega_{1,2}(k) = -2ik^2 \pm \left[\frac{1}{2}(H-8)k^4 - \gamma H k^2\right]^{1/2}. \tag{3.9}$$

Because of symmetry, one needs to consider $\mathrm{Re}(k) > 0$ only in the temporal stability analysis. Furthermore, only one of the branches, say $\omega_1(k)$, can have values with positive imaginary parts for real wavenumbers. The range of unstable wavenumbers is the single interval

$$0 < k < (2\gamma)^{1/2}. \tag{3.10}$$

Thus, any disturbance with a sufficiently short wavelength decays in time, and the temporal stability analysis is compatible with the long-wave assumption. The maximum temporal growth rate is

$$G_0 \equiv \max_{0<k<(2\gamma)^{1/2}}\{\mathrm{Im}[\omega_1(k)]\} = \frac{\gamma H}{\sqrt{2}(H^{1/2} + 2\sqrt{2})}, \tag{3.11}$$

which is reached for

$$k_0 = \left(\frac{\gamma H^{1/2}}{H^{1/2} + 2\sqrt{2}}\right)^{1/2}. \tag{3.12}$$

The film life time T can be estimated from

$$|h'(x,T)| = \frac{1}{2}H. \tag{3.13}$$

Equations (3.11) and (3.13) give

$$|h'(x,t)| = |\tilde{h}|\exp(G_0 t), \tag{3.14}$$

$$T = G_0^{-1}\log\left(\frac{1}{2}H|\tilde{h}|^{-1}\right). \tag{3.15}$$

3.2. Development of localized disturbances

A small disturbance is produced at $t = 0$ in the form of finite integrable functions $u'(x,0)$ and $h'(x,0)$. The solution of (3.2) and (3.3) can then be expressed as the double Fourier integrals

$$h'(x,t) = \frac{1}{4\pi^2}\int_{-\infty}^{+\infty}\int_C \frac{\Phi(k,\omega)\exp(ikx - i\omega t)}{D(k,\omega)}d\omega dk, \tag{3.16}$$

$$u'(x,t) = \frac{1}{4\pi^2}\int_{-\infty}^{+\infty}\int_C \frac{\Psi(k,\omega)\exp(ikx - i\omega t)}{D(k,\omega)}d\omega dk, \tag{3.17}$$

in which the integration contour C in the complex ω plane is a horizontal line that is located above all the singularities of the integrand, $D(k,\omega)$ is given by the dispersion relation (3.6), and

$$\Phi(k,\omega) \equiv i(\omega + 4ik^2)\,\hat{h}(k) + iHk\hat{u}(k), \tag{3.18}$$

$$\Psi(k,\omega) \equiv ik\left(\frac{1}{2}k^2 - \gamma\right)\hat{h}(k) + i\omega\hat{u}(k) \tag{3.19}$$

with

$$\hat{h}(k) = \int_{-\infty}^{+\infty} h'(x,0)\exp(-ikx)\,dx \tag{3.20}$$

and

$$\hat{u}(k) = \int_{-\infty}^{+\infty} u'(x,0)\exp(-ikx)dx \tag{3.21}$$

being the Fourier transforms of the initial conditions.

The asymptotic behaviour of the disturbances for $t \to +\infty$ is studied along a trajectory defined in the (x,t) plane as $x = Ut$, in which U is an appropriate velocity. If the Doppler-shifted frequency is introduced as $\Omega = \omega - Uk$, (3.6) and (3.16) give, respectively,

$$\Omega_{1,2}(k) = -Uk - 2ik^2 \pm \left[\frac{1}{2}(H-8)k^4 - \gamma Hk^2\right]^{1/2} \tag{3.22}$$

and

$$h'(Ut,t) = \frac{1}{4\pi^2}\int_{-\infty}^{+\infty}\int_C \frac{\Phi(k,\Omega+Uk)\exp(-i\Omega t)}{D(k,\Omega+Uk)}\,d\Omega dk. \tag{3.23}$$

If the integration with respect to Ω is performed first, (3.23) gives for $t > 0$

$$h'(Ut,t) = -\frac{i}{2\pi}\int_{-\infty}^{+\infty}\sum_{p=1,2}\frac{\Phi[k,\Omega_p(k)+Uk]\exp[-i\Omega_p(k)t]}{D_\omega[k,\Omega_p(k)+Uk]}dk, \tag{3.24}$$

in which $D_\omega(k,\omega)$ is the ω-derivative of the dispersion relation (3.6).

The origin of the complex k plane is a double branch point of the frequency, for which $\mathrm{Im}[\Omega_{1,2}(0)] = 0$. In addition, two other branch points occur at

$$k^b_{1,2} = \pm\left(\frac{2\gamma H}{H-8}\right)^{1/2}, \tag{3.25}$$

which are either real or complex conjugates. At the branch points, the denominators of both terms in (3.24) are zero, yet the singularities neutralize each other. Thus, the terms can be investigated independently only if the integration contours pass distantly from the branch points.

If the integration contour for each term can be continuously deformed from the real k axis to a curve such that $\mathrm{Im}[\Omega_p(k)] \le 0$ and if zero values are reached at isolated points, then $h'(Ut,t) \to 0$ as $t \to +\infty$. The obstacles to the deformation are saddle points k^s that are zeros of the group velocity

$$\frac{d\Omega_p}{dk}(k^s) = 0. \tag{3.26}$$

In addition, the so-called "pinching requirement" must be satisfied, *i.e.* the corresponding branch points on the complex Ω plane must connect two branches of the wavenumber which have opposite signs of $\mathrm{Im}[k(\Omega)]$ for large $\mathrm{Im}(\Omega) > 0$ (e.g. Akhiezer and Polovin, 1971). In many cases, the proper saddle points can be chosen from the geometric consideration of the contour plots of $\mathrm{Im}[\Omega_p(k)]$ in the complex k plane. In the general case, a special mapping procedure can be utilized (Kupfer *et al.*, 1987).

Because of symmetry, it is sufficient to consider only $U > 0$, $\mathrm{Re}(k) > 0$, and the "unstable" temporal branch $\Omega_1(k)$. Equations (3.22) and (3.26) yield six saddle points. Two of them form a double saddle point at the origin, the others are solutions of the following fourth-order polynomial equation:

$$k^4 - \frac{4iU}{H}k^3 - \left(\frac{U^2}{2H} + 2\frac{\gamma H}{H-8}\right)k^2 + \frac{8iU\gamma}{H-8}k + \gamma\frac{U^2+\gamma H}{H-8} = 0. \tag{3.27}$$

The correspond branch points are

$$\Omega^b = -k^s\left(U + \frac{k^s(2iU - Hk^s) + \gamma H}{U + 4ik^s}\right). \tag{3.28}$$

If $U \ge 0$, one has $\mathrm{Re}(k) > 0$ only for two of the solutions of (3.27). For $U = 0$, they are

$$k^s_\pm = \left(\frac{\gamma H^{1/2}}{H^{1/2} \pm 2\sqrt{2}}\right)^{1/2}; \tag{3.29}$$

the corresponding branch points are

$$\Omega^b_\pm = \frac{i\gamma H}{\sqrt{2}\,(2\sqrt{2} \pm H^{1/2})}. \tag{3.30}$$

Note that $k^s_+ = k_0$ is given by (3.12). Two topologically different cases occur.

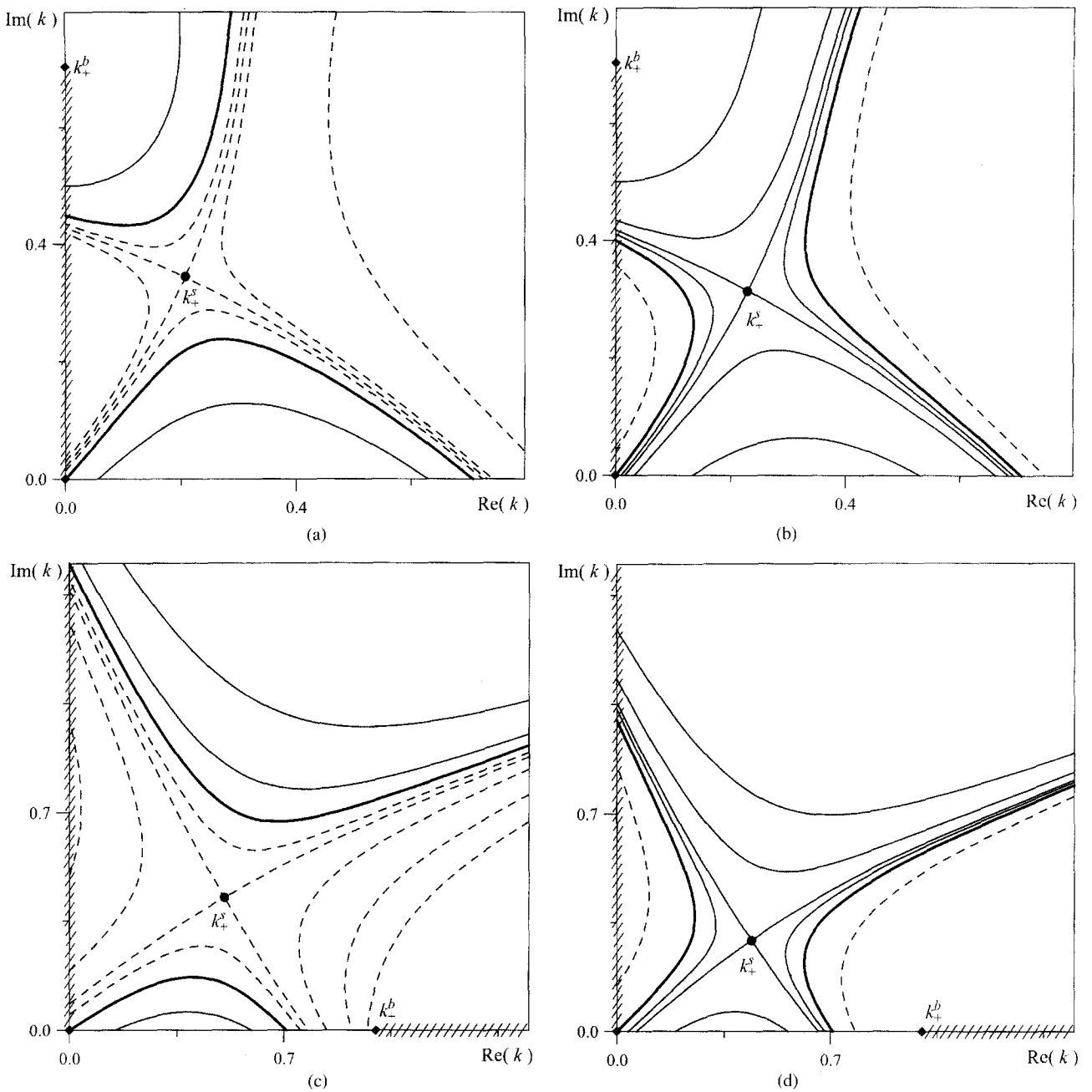

Fig. 1. – Contour plots of $\mathrm{Im}[\Omega_1(k)]$ for $\gamma = 0.25$ and for (a) $H = 4$, $U = 0.9$; (b) $H = 4$, $U = 0.8$; (c) $H = 16$, $U = 3$; (d) $H = 16$, $U = 2$. The solid, dashed, and bold lines and for positive, negative, and zero values, respectively. The branch cuts are shown by the hatched lines.

If $H > 8$, both branch points $\Omega^b_{\pm}$ connect two spatial branches that originate from opposite halves of the complex k plane. However, between two corresponding saddle points, only k^s_+ belongs to the unstable branch of the frequency $\Omega_1(k)$, as shown in Figure 1(a, b). Thus, one always has $\mathrm{Im}(\Omega^b_-) < 0$.

If $H < 8$, the saddle point k^s_- is located close to the positive half of the imaginary k axis, and the branch point Ω^b_- connects two spatial branches that originate from the same upper half-plane. Therefore, the saddle

point k_-^s has not to be taken into account, and the asymptotic behaviour of the disturbance is determined completely by the saddle point k_+^s, as shown in Figure 1(*c*, *d*).

The loci of $k_+^s(U)$ in the complex k plane are displayed in Figure 2. Since $\mathrm{Re}\,(k_+^s)$ remains finite, the integration in (3.24) can be truncated for large k, which validates the compatibility with the long-wave approach.

The growth rate of the disturbance along the ray $x = Ut$ is

$$G_{\mathrm{abs}}(U) \equiv \mathrm{Im}[\Omega_+^b(U)]. \tag{3.31}$$

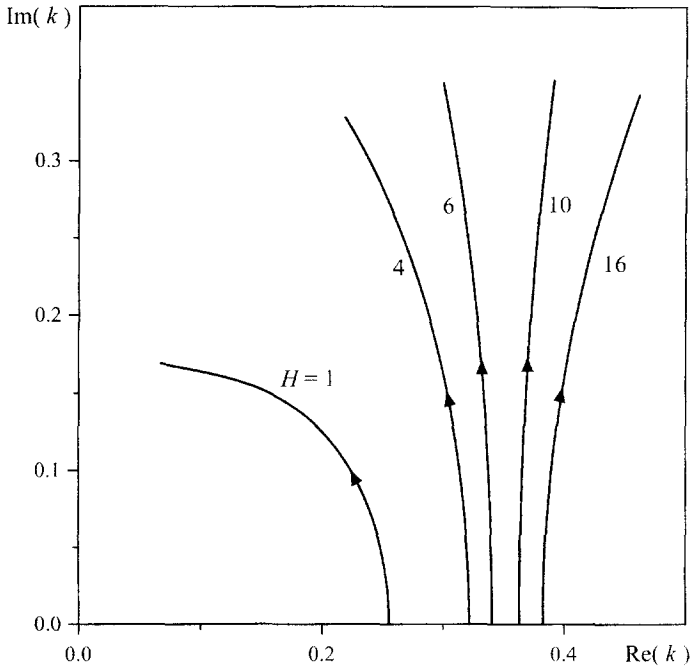

Fig. 2. – Loci of the saddle point $k_+^s(U)$ as U increases from zero to $U_{\max}$ for $\gamma = 0.25$ and different values of the undisturbed film thickness.

In the frame of reference moving with the speed U, it corresponds to the "absolute growth rate" (e.g. Huerre and Monkewitz, 1990). One has

$$\max_U [G_{\mathrm{abs}}(U)] = G_{\mathrm{abs}}(0) = G_0 \tag{3.32}$$

that is the temporal growth rate given by (3.11). The disturbance decays in time along any ray $x = Ut$ such that

$$U > U_{\max}(\gamma, H), \tag{3.33}$$

which gives the speed of the disturbance edges.

The method of steepest descent applied to (3.24) gives the following estimate as $t \to +\infty$:

$$h'(Ut, t) \sim a(U) t^{-1/2} \exp[-i\Omega_+^b(U)t], \tag{3.34}$$

in which

$$a = -\exp\left(\frac{i\pi}{4}\right) \frac{\Phi\,(k_+^s, \Omega_+^b)}{D_\omega(k_+^s, \Omega_+^b + U k_+^s)} \left[2\pi \frac{d^2\Omega_1}{dk^2}(k_+^s)\right]^{-1/2}. \tag{3.35}$$

The estimate given by (3.34) is valid only if time is sufficiently large. Due to (3.32), one then has

$$\max_U[|h'(Ut,t)|] = |h'(0,t)| = |a(0)|t^{-1/2}\exp(G_0 t), \tag{3.36}$$

in which t is a parameter. From (3.13) and (3.36), the film life time can be estimated as

$$T = -\frac{W_{-1}(-8|a|^2 H^{-2} G_0)}{2\,G_0}, \tag{3.37}$$

in which W_{-1} is the Lambert function (Corless *et al.*, 1996). The life time given by (3.37) is larger than that obtained from the temporal theory, Eq. (3.15). Actually, if $|\tilde{h}| \sim |a(0)|$, (3.36) differs from (3.14) only by the factor $t^{-1/2}$.

Numerical studies by Sharma *et al.* (1995) based on the non-linear evolution of disturbances have shown that disturbances grow explosively at later stages. Thus, the linear theory always overestimates the film lifetime (Figs. 5–8, p. 1839 of Sharma *et al.*, 1995).

3.3. Example

If the disjoining pressure is related to the potential of van der Waals forces, the following dimensionless form can be used

$$\Pi(h) = -Ah^{-3}, \tag{3.38}$$

in which the dimensionless constant $A > 0$ is proportional to the Hamaker constant. Equation (3.4) gives

$$\gamma = 3\,AH^{-4}. \tag{3.39}$$

Then, the interval of "unstable" wavenumbers is

$$0 < k < (6A)^{1/2}\,H^{-2}, \tag{3.40}$$

the most amplified wavenumber is

$$k_0 = \left(\frac{3AH^{-7/2}}{H^{1/2} + 2\sqrt{2}}\right)^{1/2}, \tag{3.41}$$

and the maximum temporal growth rate is

$$G_0 = \frac{3AH^{-3}}{\sqrt{2}\,(2\sqrt{2} \pm H^{1/2})}. \tag{3.42}$$

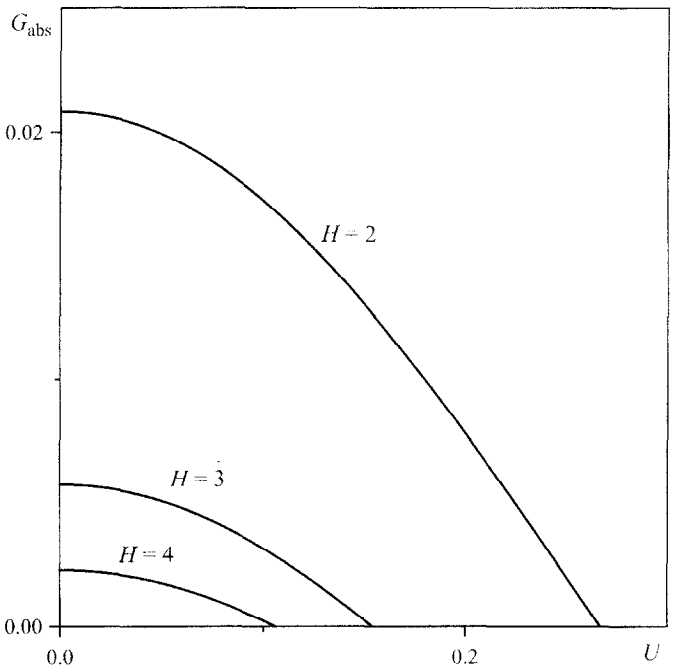

Fig. 3. – Growth rates of disturbances along the rays $x = Ut$ for different values of the undisturbed film thickness.

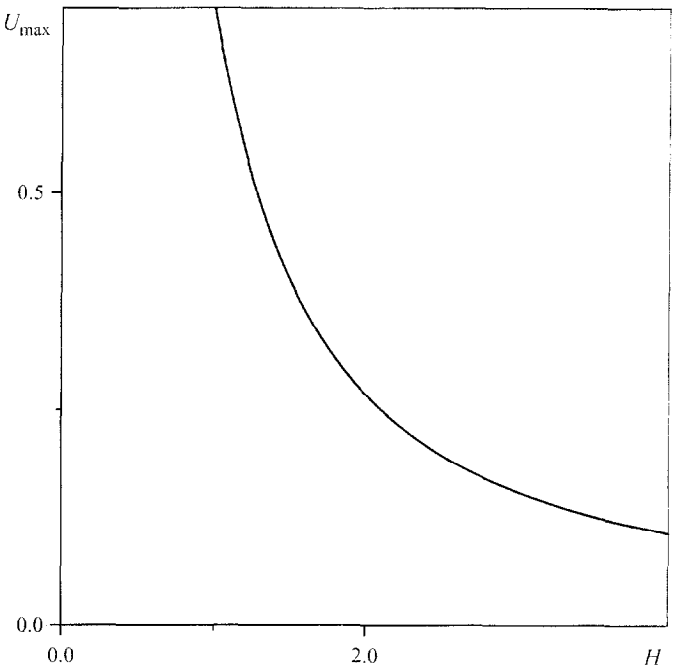

Fig. 4. – Speed of the edges of a localized disturbance vs. thickness of the undisturbed film.

To demonstrate qualitatively how the absolute growth rate $G_{\rm abs}(U)$ and the spreading speed of the disturbance $U_{\rm max}$ vary with H, one can assign any value to A. For example, setting $A = 1/3$ entails no loss of generality. The results are presented in Figures 3 and 4. Thus, both $G_{\rm abs}(U)$ and $U_{\rm max}$ increase as H decreases.

4. Conclusions and discussion

Spatio-temporal stability analysis of a free ultra-thin film of viscous liquid shows that even in the linear approximation, the long-range intermolecular forces strongly affect the evolution of initially localized disturbances. The analysis is based on the linearization of the long-wave evolution equations of Erneux and Davis (1993), which are rewritten in an equivalent form that utilizes the disjoining pressure.

The present approach is based on the analysis of the asymptotic behaviour of the wave packet solution to the initial value problem. It is more general and, perhaps, more realistic than the normal mode stability analysis. A negative disjoining pressure that is caused by van der Waals attraction strongly promotes instability. Thus, as the thickness of the undisturbed film decreases, both the absolute growth rate and speed of spreading of disturbances increase.

The estimated time of the film rupture is larger than that found from linear temporal stability analysis. As noted by Sharma *et al.* (1995), linear theory always overestimates the film life time. This overestimation is mostly due to the explosive non-linear growth of disturbances at later stages of evolution. However, close to the onset of rupture, the film is too thin to be described adequately even by a non-linear continuum theory. A completely alternative approach is based on kinetic theory (e.g. Koplik and Banaver, 1993). However, it typically requires extensive numerical computations.

Acknowledgements

The authors thank K. G. Kornev for calling their attention to this problem and for many useful discussions.

This work was supported by The Royal Swedish Academy of Sciences (Project no. 1264).

APPENDIX

Derivation of the basic equations

In this appendix, a pair of equations for the film thickness and velocity is derived asymptotically from the Navier-Stokes equations. Although the final form of these equations is similar to that obtained by ED, the derivation procedure is not completely the same. First of all, the assumption of symmetric disturbances appears to be not necessary *a priori*, since this restriction is obtained automatically to within the leading order approximation. In addition, the disjoining pressure is used instead of the van der Waals potential.

In the scaled dimensionless variables given by (2.3) and (2.4), the continuity equation and navier-Stokes equations take the form

$$\frac{\partial u}{\partial x} + \frac{\partial v}{\partial y} = 0, \tag{A.1}$$

$$\frac{\partial u}{\partial t} + u\frac{\partial u}{\partial x} + v\frac{\partial u}{\partial y} = -\frac{\partial p}{\partial x} + \varepsilon^{\alpha}\left(\frac{\partial^2 u}{\partial x^2} + \frac{1}{\varepsilon^2}\frac{\partial^2 u}{\partial y^2}\right). \tag{A.2}$$

$$\frac{\partial v}{\partial t} + u\frac{\partial v}{\partial x} + v\frac{\partial v}{\partial y} = -\frac{1}{\varepsilon^2}\frac{\partial p}{\partial y} + \varepsilon^{\alpha}\left(\frac{\partial^2 v}{\partial x^2} + \frac{1}{\varepsilon^2}\frac{\partial^2 v}{\partial y^2}\right). \tag{A.3}$$

At the film surfaces $y = \zeta^{\pm}(x,t)$, the kinematic condition requires that

$$v = \frac{\partial \zeta^{\pm}}{\partial t} + u\frac{\partial \zeta^{\pm}}{\partial x}, \tag{A.4}$$

and the tangential and normal stress balances give, respectively,

$$\left(\frac{\partial u}{\partial y} + \varepsilon^2 \frac{\partial v}{\partial x}\right)\left[1 - \varepsilon^2\left(\frac{\partial \zeta^{\pm}}{\partial x}\right)^2\right] - 4\varepsilon^2 \frac{\partial \zeta^{\pm}}{\partial x}\frac{\partial u}{\partial x} = 0 \tag{A.5}$$

and

$$\begin{aligned} -p - 2\varepsilon^{\alpha}\left\{\frac{\partial u}{\partial x}\left[1 - \varepsilon^2\left(\frac{\partial \zeta^{\pm}}{\partial x}\right)^2\right] + \frac{\partial \zeta^{\pm}}{\partial x}\left(\frac{\partial u}{\partial y} + \varepsilon^2\frac{\partial v}{\partial x}\right)\right\} \times \\ \times\left[1 + \varepsilon^2\left(\frac{\partial \zeta_1^{\pm}}{\partial x}\right)^2\right] = \pm\varepsilon^{2\alpha}\frac{\partial^2 \zeta^{\pm}}{\partial x^2}\left[1 + \varepsilon^2\left(\frac{\partial \zeta^{\pm}}{\partial x}\right)^2\right]^{-3/2} + \Pi(h), \end{aligned} \tag{A.6}$$

in which $h = \zeta^{+} - \zeta^{-}$ is the film thickness, and $\Pi(h)$ is the disjoining pressure that is made dimensionless by ρV_x^2.

If the following series expansions are applied

$$\{u, v, p, h, \zeta^{\pm}\} = \sum_{j=0}^{\infty} \varepsilon^{(2-\alpha)j}\{u_j, v_j, p_j, h_j, \zeta_j^{\pm}\}, \tag{A.7}$$

(A.1) and (A.2) yield

$$\frac{\partial u_0}{\partial x} + \frac{\partial v_0}{\partial y} = 0, \tag{A.8}$$

$$\frac{\partial^2 u_0}{\partial y^2} = 0. \tag{A.9}$$

The boundary conditions (A.4) and (A.5) give at $y = \zeta_0^{\pm}$

$$v_0 = \frac{\partial \zeta_0^{\pm}}{\partial t} + u_0\frac{\partial \zeta_0^{\pm}}{\partial x}, \tag{A.10}$$

$$\frac{\partial u_0}{\partial y} = 0. \tag{A.11}$$

Equation (A.9) together with the boundary condition (A.11) lead to

$$u_0 = u_0(x,t). \tag{A.12}$$

Hence, to order ε^0, the velocity profile is uniform across the film. The continuity equation (A.8) implies that $\partial^2 v_0/\partial y^2 = 0$. Then, (A.3) gives $\partial p_0/\partial y = 0$. Therefore, to within the same approximation order, the pressure is also constant across the film.

The continuity equation (A.8) integrated from $y = \zeta_0^-$ to $y = \zeta_0^+$ together with the boundary conditions (A.10) give Eq. (2.6).

To proceed further with the asymptotic analysis, one needs an additonal assumption about α.

If $\alpha = 0$, (A.6) and (A.8) imply that

$$\frac{\partial^2 \zeta_0^+}{\partial x^2} = -\frac{\partial^2 \zeta_0^-}{\partial x^2} = \frac{1}{2}\frac{\partial^2 h_0}{\partial x^2}, \tag{A.13}$$

$$p_0 = -\Pi(h_0) - 2\frac{\partial u_0}{\partial x} - \frac{1}{2}\frac{\partial^2 h_0}{\partial x^2}. \tag{A.14}$$

Equation (A.13) indicates that only symmetric disturbances (squeezing modes) can be sudied in the leading order approximation.

At second order in ϵ, (A.3) yields

$$\frac{\partial^2 u_1}{\partial y^2} = \frac{\partial u_0}{\partial t} + u_0\frac{\partial u_0}{\partial x} + \frac{\partial p_0}{\partial x} - \frac{\partial^2 u_0}{\partial x^2}, \tag{A.15}$$

and the boundary condition (A.5) together with (A.12) give at $y = \zeta_0^{\pm}$

$$\frac{\partial u_1}{\partial y} = 4\frac{\partial \zeta_0^{\pm}}{\partial x}\frac{\partial u_0}{\partial x} - \frac{\partial v_0}{\partial x}. \tag{A.16}$$

The continuity equation (A.8) differential with respect to x and integrated from $y = \zeta_0^-$ to $y = \zeta_0^+$ leads to:

$$\left.\frac{\partial v_0}{\partial x}\right|_{y=\zeta_0^+} - \left.\frac{\partial v_0}{\partial x}\right|_{y=\zeta_0^-} = -h\frac{\partial^2 u_0}{\partial x^2}. \tag{A.17}$$

Equation (A.15) integrated from $y = \zeta_0^-$ to $y = \zeta_0^+$ together with the boundary conditions (A.16), (A.14) and (A.17) finally yield Eq. (2.7).

If $\alpha > 0$, Equations (A.11), (A.6) and (A.3) give straightforwardly $p_0 = -\Pi(h_0)$ and thus Eq. (2.8).

REFERENCES

AKHIEZER A. I., POLOVIN R. V., 1971, Criteria for wave growth, *Sov. Phys. Usp.*, **14**, 278–285.

CHANG H.-C., 1994, Wave evolution on a falling film. *Annu. Rev. Fluid Mech.*, **26**, 103–136.

CORLESS R. M., GONNET G. H., HARE D. E. G., JEFFREY D. J., KNUTH D. E., 1996, On the Lambert W function, *Adv. Comput. Math.*, **5**, 529–359.

DE LUCA L., COSTA M., 1997, Instability of a spatially developing liquid sheet, *J. Fluid. Mech.*, **331**, 127–144.

DE WIT A., GALLEZ D., CHRISTOV C. I., 1994, Nonlinear evolution equations for thin liquid films with insoluble surfactants, *Phys. Fluids*, **6**, 3256–3266.

DERYAGIN B. V., 1955, The definition and magnitude of disjoining pressure and its role in the statics and dynamics of thin liquid films, *Colloid J. USSR*, **17**, 207.

DZYALOSHINSKII I. E., PITAEVSKII L. P., 1960, Van der Waals forces in liquid films, *Sov. Phys. JETP*, **10**, 161.

ERNEUX T., DAVIS S. H., 1993, Nonlinear rupture of free films, *Phys. Fluids A*, **5**, 1117–1122.

FELDERHOF B. U., 1968, Dynamics of free liquid films, *J. Chem. Phys.*, **49**, 44–51.

HOWELL P. D., 1996, Models for thin viscous sheets, *Eur. J. Appl. Math.*, **7**, 321–343.

HUERRE P., MONKEWITZ P. A., 1990, Local and global instabilities in spatially developing flows, *Annu. Rev. Fluid Mech.*, **22**, 473–537.

KOPLIK J., BANAVER J. R., 1993, Molecular dynamics of interface rupture, *Phys. Fluids A*, **5**, 521–536.

KUPFER K., BERS A., RAM A. K., 1987, The cusp map in the complex-frequency plane for absolute instability, *Phys. Fluids*, **30**, 3075–3082.

LI X., TANKIN R. S., 1991, On the temporal instability of a two-dimensional liquid sheet, *J. Fluid Mech.*, **226**, 425–118.

LI X., 1993, Spatial instability of plane liquid sheets, *Chem. Eng. Sci.*, **48**, 2973–2981.

LIN S. P., 1981, Stability of a viscous liquid curtain, *J. Fluid Mech.*, **104**, 111–118.

LIN S. P., LIAN Z. W., CREIGHTON B. J., 1990, Absolute and convective instability of a liquid sheet, *J. Fluid Mech.*, **229**, 673–689.

MALDARELLI C., JAIN R. K., 1988, The hydrodynamic stability of thin films, in *Thin Liquid Films* (Ivanov I. B., Ed.), Marcel Dekker, Inc., New York, Chap. 8.

MALDARELLI C., JAIN R. K., IVANOV I. B., RUCKENSTEIN E., 1980, Stability of symmetric and unsymmetric thin liquid films to short and long wavelength perturbations, *J. Colloid Interface Sci.*, **78**, 118–143.

RAMASWAMY S., CHIPPADA S., JOO S. W., 1996, A full-scale numerical study of interfacial instabilities in thin-film flows, *J. Fluid Mech.*, **325**, 163–194.

RUCKENSTEIN E., JAIN R. K., 1974, Spontaneous rupture of thin liquid films, *J. Chem. Soc. Faraday Trans.* II, **70**, 132–147.

SHARMA A., KISHORE C. S., SALANIWAL S., RUKENSTEIN E., 1995, Non-linear stability and rupture of ultrathin free films, *Phys. Fluids*, **7**, 1832–1840.

(Manuscript received June 16, 1997;
revised November 8, 1997;
accepted February 3, 1998.)